Seismic vibration control for bridges with high-piers in Sichuan-Tibet Railway

Zhaowei Chen[*1,2], Zhaoling Han[3], Hui Fang[4] and Kai Wei[2]

[1]School of Mechanotronics & Vehicle Engineering, Chongqing Jiaotong University, Chongqing, China
[2]MOE Key Laboratory of High-speed Railway Engineering, Southwest Jiaotong University, Chengdu, China
[3]State Key Laboratory of Traction Power, Southwest Jiaotong University, Chengdu, China
[4]Electric Power Research Institute, State Grid Chongqing Electric Power Company, Chongqing, China

Abstract.   Aiming at widely used high-pier bridges in Sichuan-Tibet Railway, this paper presents an investigation to design and evaluate the seismic vibration reduction effects of several measures, including viscous damper (VD), friction pendulum bearing (FPB), and tuned mass damper (TMD). Primarily, according to the detailed introduction of the concerned bridge structure, dynamic models of high-pier bridges with different seismic vibration reduction (SVR) measures are established. Further, the designs for these SVR measures are performed, and the optimal parameters of these measures are investigated. On this basis, the vibration reduction effects of these measures are analyzed and assessed subject to actual earthquake excitations in Wenchuan Earthquake (M=8.0), and the most appropriate SVR measure for high-pier bridges in Sichuan-Tibet Railway is determined at the end of the work. Results show that the height of pier does not obviously affect the performances of the concerned SVR measures. Comprehensively considering the vibration absorption performance, installation and maintenance of all the employed measures in this paper, TMD is the best one to absorb vibrations induced by earthquakes.

Keywords: high-pier bridge; Sichuan-Tibet Railway; seismic effect; vibration reduction; TMD

1. Introduction

As one of the most important railways planned in "Integrated Transportation System Planning in the Twelfth Five-year" enacted by the Chinese government in 2012, Sichuan-Tibet Railway is actually under construction now, which connects two big cities of Chengdu and Lhasa in Southwest China. The railway crosses the collision zone of the Indian Plate and the Eurasian Plate, and also traverses many fault zones (seen in Fig. 1), indicating that the effect of earthquake on this railway must be considered seriously. Moreover, due to numerous great mountains and deep valleys along Sichuan-Tibet Railway, a large number of bridges with high-piers are used. Compared with short-pier bridges, the high-pier bridges have poorer stability (Ceravolo *et al.* 2009). Hence, it is very meaningful and important to study vibration reduction for high-pier bridges subject to earthquake loadings in Sichuan-Tibet Railway.

Recently, many seismic vibration reduction (SVR) measures are proposed in railway engineering, which are effective to reduce structural vibrations. In China, viscous damper (VD), friction pendulum bearing (FPB), and tuned mass damper (TMD) are the most widely adopted measures to reduce seismic vibrations of railway bridges, and the authors were commissioned to determine the most appropriate SVR measure for high-pier bridges in Sichuan-Tibet Railway. On this basis, the vibration reduction performances of these three measures are designed,

assessed and compared in this present work.

VD is a traditional, simple vibration absorption measure, which has been widely used to control structural vibrations around the world (Hüffmann 1985, Veletsos and Ventura 1986, Buckle and Mayes 1990). The effectiveness of VD in reducing bridge vibrations has also been validated in many literatures (Pacheco *et al.* 1993, Main and Jones 2002). After years of development, the design methodology and application technology of VD have been very mature. Moreover, from the above investigations, VD has some remarkable advantages, including providing a large damping to a certain primary structure, working non-linearly in broad frequency ranges, insensitivity to temperature, and so on. While the drawback is also obvious, such as machining difficulty and liquid leakage.

FPB was first manufactured by Earthquake Protection Systems, Inc. (EPS) in 1985 (Zhuang 2012), and firstly used in bridges and buildings in United States and Japan (Buckle 1986, Kelly 1988). Until now, this technique has been extensively applied to absorb structural vibrations subject to earthquakes. The device is able to recenter by itself and dissipate a lot of energy through the sliding motions on the curved surface (Landi *et al.* 2016). The spherical-shape sliding surface is the most important part in a FPB, whose mechanical behavior directly affects the dynamic performance of FPB, thus, many studies paid attention to sliding surfaces and lots of beneficial suggestions were proposed (Zayas *et al.* 1987, Mokha *et al.* 1990, Fenz and Constantinou 2006, Landi *et al.* 2016). From these studies, several notable conclusions were reached: (a) the mechanics behavior of FPB is bilinear, (b) FPB is effective to reduce seismic vibrations of structures, (c) parameters of FPB are quantifiable, and (d) numerical

---

*Corresponding author, Ph.D.
E-mail: chenzhaowei_cq@163.com
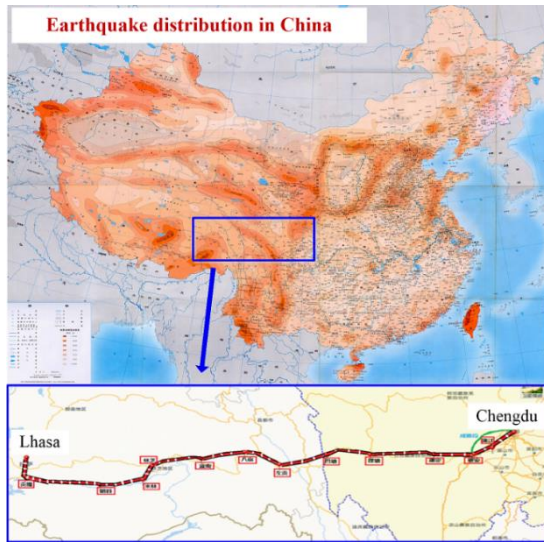
Fig. 1 Basic situation of Sichuan-Tibet Railway

(a) 32.6 m-long T-beam bridges

(b) Cross section of the beam
Fig. 2 The 32.6 m-long T-beam bridges

(a) High piers   (b) Structure of the pier
Fig. 3 Hollow high piers
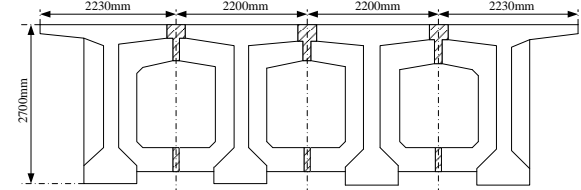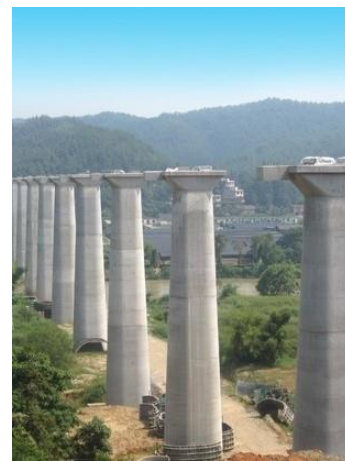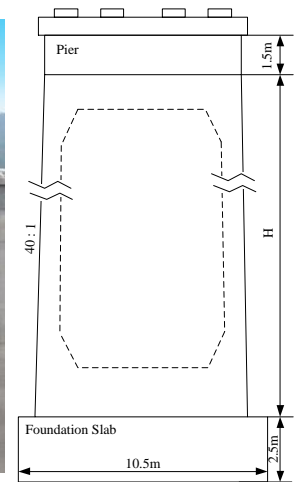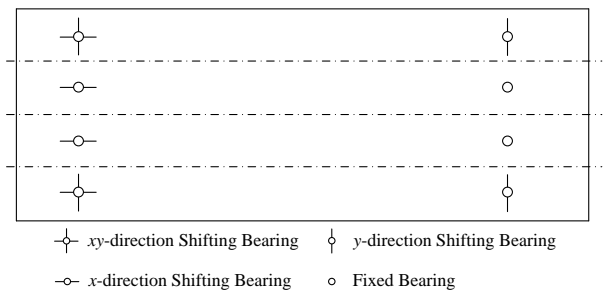

Fig. 4 Arrangement of the bearings

analysis techniques are available to investigate the dynamic behaviours of FPB.

Moreover, TMD is another simple, effective, inexpensive and reliable measure to absorb structural vibrations. As early as 1928, Ormondroyd (1928) pointed out that a vibration absorber with damping was effective to control structural vibrations caused by variable-frequency forces. Five years later, Erich Hahnkamm (1933) revealed that two fixed points existed in designing a TMD. Based on the mechanics characteristics of the two fixed points, i.e., the fix-point principle, the expressions of the optimal stiffness and mass ratio were deduced. On this basis, the expression of optimal damping was derived by Brock (1946). Afterwards, Den Hartog (1956) systematically pointed out the optimal mass ratio, stiffness and damping in his book. Since then, the basic theory of designing a TMD for a certain dynamic system has been established, and it has also been widely adopted to reduce structural vibrations subject to earthquake loadings in bridge engineering (Sladek and Klingner 1983, Soto-Brito and Ruiz 1999, Quaranta *et al.* 2016). TMD is simple and effective, while its drawbacks limit its wider applications, such as the sensitivity to frequency and the influence on primary structure as an additional mass (Zhu *et al.* 2017b).

Although many existing literatures have done works on vibration reduction for bridge structures adopting these above SVR measures, few researchers paid attention to reduce seismic vibrations of bridges with high-piers, and also almost no studies compared the performances of these measures for such high-bridge structures. Hence, aiming at high-pier bridges in Sichuan-Tibet Railway, this paper designs, evaluates and compares the SVR performances of VD, FPB, and TMD. On this basis, the most appropriate measure for reducing seismic responses of high-pier bridges in Sichuan-Tibet Railway is investigated. Primarily, the concerned high-pier bridge is briefly introduced in Part 2. Further, the dynamic models of the high-pier bridges with different SVR measures are established in Part 3, and the optimal parameters for these adopted measures are calculated in Part 4. In the last part, the SVR performances

of all these three measures are assessed and compared, and the most appropriate one for high-pier bridges in Sichuan-Tibet Railway is determined.

2. Research object

According to the design drawings of Sichuan-Tibet Railway, 32.6 m-long T-beam bridges are most widely used in this railway. For example, in the Lhasa-Nyingchi section, 32.6 m-long T-beam bridges occupy a proportion of 93%
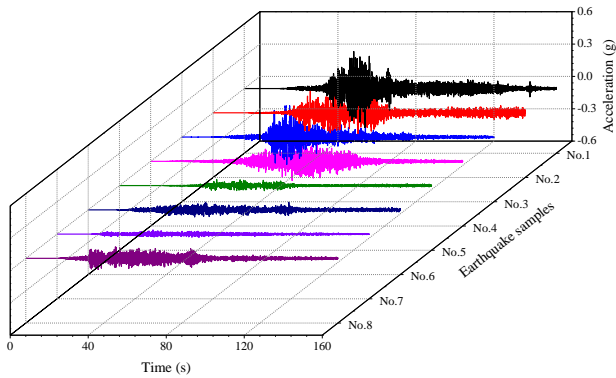
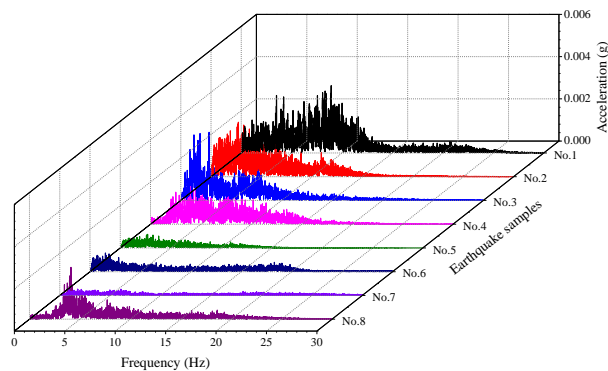Fig. 5 Earthquake samples of the Wenchuan Earthquake in time-domain

Fig. 6 Earthquake samples in frequency-domain

Table 1 Details of the concerned earthquake samples

Earthquake samples	Amplitude	Dominant frequency range
No. 1	0.36 g	3.5 Hz-5 Hz, 6.5 Hz-13 Hz
No. 2	0.23 g	0.5 Hz-6.5 Hz
No. 3	0.29 g	0.5 Hz-3 Hz, 4.5 Hz-8 Hz
No. 4	0.25 g	2.5 Hz-6.4 Hz, 7.2 Hz-10.4 Hz
No. 5	0.058 g	0.2 Hz-5 Hz
No. 6	0.069 g	0.15 Hz-3.6 Hz, 16 Hz-21 Hz
No. 7	0.037 g	0.2 Hz-6.5 Hz, 12 Hz-18 Hz
No. 8	0.106 g	3 Hz-6.5 Hz

among all bridge structures (Geology Institute of China Earthquake Administration 2013). Considering this practical situation, in this study, the standard 32.6 m-long T-beam bridge (as shown in Fig. 2) with hollow high-piers (as illustrated in Fig. 3) is adopted as the research object, and three height levels are selected, including 40 m, 50 m, and 60 m. In addition, 8 bearings are arranged in this bridge system according to the actual design drawings, as shown in Fig. 4. The secondary dead load is set to be 160 kN/m according to the actual weight of the structures including the track and other accessory structures.

To make the following calculations more approximated to the real conditions in Sichuan-Tibet Railway, 8 different actual earthquake samples of the Wenchuan Earthquake (*M*=8.0) in 2008 nearby Sichuan-Tibet Railway are selected, which are acquired by different seismic

monitoring stations in Southwest China, as shown in Figs. 5-6. As seen from these figures, the amplitudes, the durations and the dominant frequencies of these 8 earthquakes are all different, further, the details of these earthquake samples are listed in Table 1.

It should be noted that earthquakes in lateral direction harm the bridge structures severely, and the bridges with high-piers are unstable under excitations along lateral direction. In this aspect, the goal of this present work is to control seismic vibrations of high-pier bridges in lateral direction.

3. Dynamic models of high-pier bridges adopting different SVR measures

Employing the finite element software ANSYS, the bridge models are built, as seen in Fig. 7. The following issues are considered in the models:

(a) The bridge beams and the high-piers are built with element BEAM188. This element is a type of spatial Timoshenko-Beam element with 6 DOFs for each node, which is widely used in bridge modelling (Timoshenko 1922, Frýba 1976, Chen *et al.* 2015). The cross sections of the beam elements are set according to Figs. 2 and 3.

(b) The height of the piers is set to be 40 m, 50 m, and 60 m, respectively.

(c) The secondary dead load is regarded as additional density of bridge beam.

(d) To eliminate the boundary effect, the number of bridge span is set to be 3.

(e) In the models with VD and TMD, the shifting bearings are simulated by linear spring-damping element COMBIN14, and VDs are modelled at all the *y*-direction shifting bearings. For the bridge models with FPB, the non-linear spring element COMBIN39 is employed due to the bilinear behaviors of FPB system.

(f) The fixed bearings are regarded as couplings of the corresponding DOFs.

(g) The base of the piers (i.e., the soil-pier interaction) is considered as springs in three translation DOFs and three rotation DOFs, and the values of the spring stiffness are set according to the actual geological conditions, as listed in Table 2 (Geology Institute of China Earthquake Administration 2013, Chen *et al.* 2016).

(h) The damping of the bridge structure is considered as Rayleigh Damping (Chen *et al.* 2018a, 2018b).

Following the above modeling principles, the high-pier bridge models are established. Further, the different SVR measures are simulated as follows, and their parameters will be calculated in the next section.

(a) VD is regarded as an external non-linear damping between the top of the pier and the bottom of the beam. The non-linear element COMBIN37, which is able to model damping as a function of velocity, is used to simulate VD;

(b) FPB is modeled by the non-linear spring element COMBIN39 because of its bilinear behavior;

(c) TMD system consists of three parts, namely a mass block, a linear spring and a damper. In the numerical simulation, the mass block is modeled with the mass element MASS21, and the spring-damper is built by the

Table 2 Spring stiffness of the soil-pier interaction

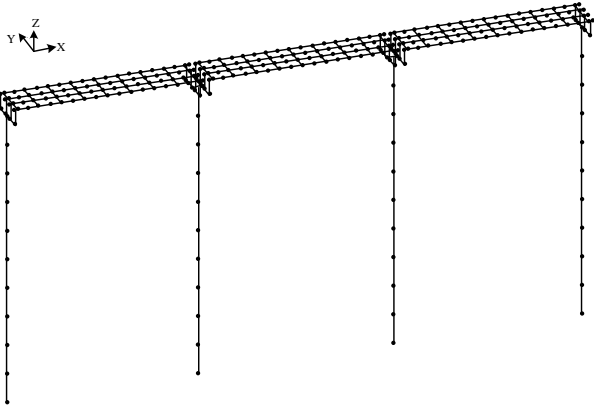| Item	Value	Unit
Stiffness along x-axle	1.5×10^9	N/m
Stiffness along y-axle	1.5×10^9	N/m
Stiffness along z-axle	2×10^{10}	N/m
Stiffness around x-axle	3×10^{11}	N·m/rad
Stiffness around y-axle	2×10^{11}	N·m/rad
Stiffness around z-axle	5×10^{10}	N·m/rad

Fig. 7 Finite element model of the high-pier bridge

element COMBIN14.

4. Design of different SVR measures

The finite element models of the high-pier bridges with different SVR measures are established in the previous section. In this part, the optimal parameters for these measures will be investigated.

In the calculations, four key bridge dynamic indicators are selected, namely the displacement of pier-top (i.e., the top of the pier), the acceleration of pier-top, the bending moment of pier-bottom (i.e., the bottom of the pier), and the stress of pier-bottom. Moreover, to uniformly describe the SVR effects, the vibration reduction rate (VRR) is defined

$$\text{VRR}(x) = \frac{\overline{x} - x}{x} \times 100\% \qquad (1)$$

in which

$$x \in \{d, a, m, s\} \qquad (2)$$

in Eqs. (1)-(2), $\overline{x}$ and x are the response amplitudes without and with vibration reduction measures, respectively. d, a, m, and s represent the displacement of pier-top, the acceleration of pier-top, the bending moment of pier-bottom, and the stress of pier-bottom, respectively.

4.1 Optimal parameters of VD

If the damping of a primary structure is not enough, the vibrations may be excessive. Thus, the most direct way to restrain vibrations is adding damping to the dynamic
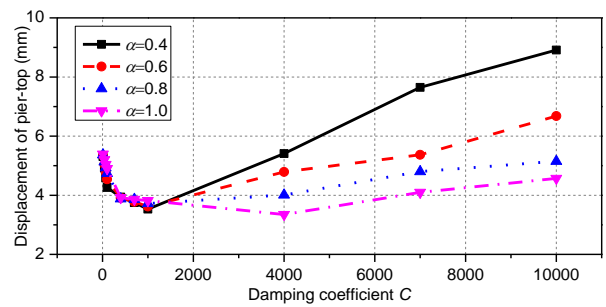

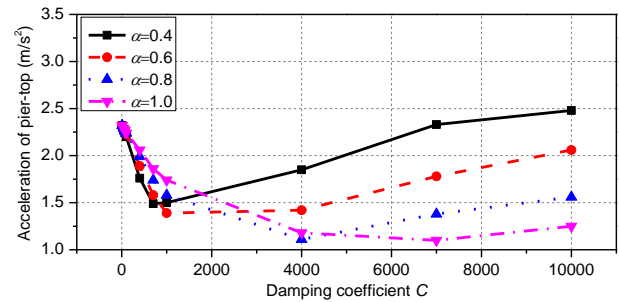(a) Installation of the damper
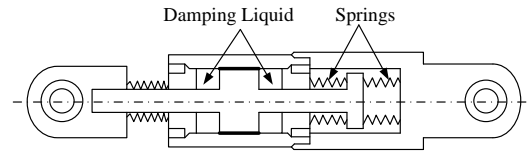
(b) Configuration of the damper

Fig. 8 Viscous damper

(a) Displacement of pier-top

(b) Acceleration of pier-top

Fig. 9 Dynamic responses of the bridge subject to the No.1 Earthquake

system, so VD (as shown in Fig. 8 (Zhuang 2012)) emerges at the right moment. VD connects the pier and the bottom of the beam body, and transfers kinetic energy of the bridge structure into thermal energy. For different dynamic systems, the optimal damping is different, therefore, an investigation is conducted to determine the optimal damping of VD for 32.6 m-long high-pier T-beam bridges.
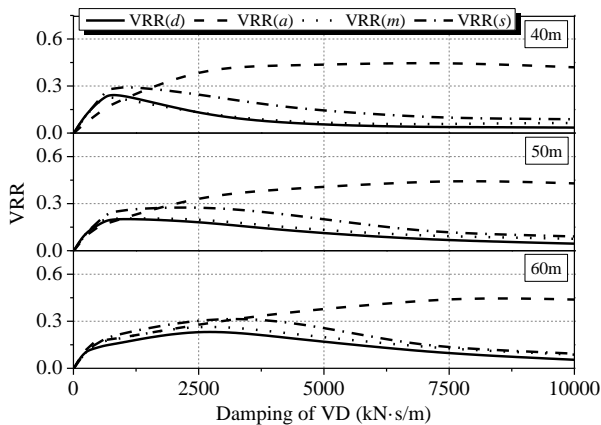
The mechanical model of VD can be expressed by

$$F_{\text{VD}} = Cv^{\alpha} \qquad (3)$$

Where F_{VD} is damping force; C is damping coefficient; v is relative velocity, and α represents damping exponent, which is in the range of 0.1-2. For VDs in bridge engineering, the value α usually varies between 0.3 and 1 (Zhuang 2012). As also seen from Eq. (3), two key parameters should be determined in designing an optimal
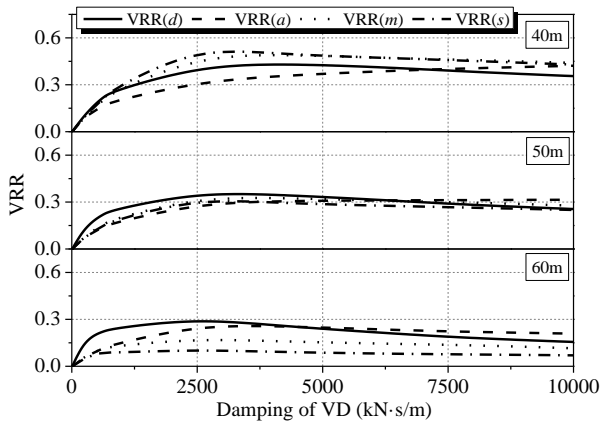
(a) Subject to No. 1 Earthquake

(b) Subject to No. 2 Earthquake

Fig. 10 Influence of the damping of VDs on VRRs

(a) Configuration of the bearing

(b) bilinear characteristic of the bearing

Fig. 11 Friction pendulum bearing
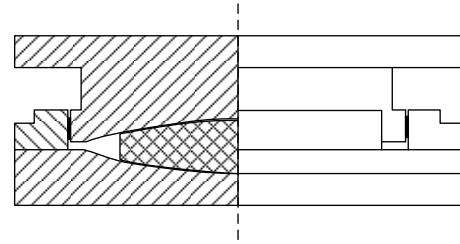
VD system, i.e., C and α.

(1) Determination of damping exponent α

Fig. 9 shows the dynamic responses of the bridge subject to the No. 1 Earthquake. As concluded from the results, for VD with a small damping coefficient, the effects of different damping exponent α are not distinguishable. However, with the increase of C, the dynamic vibrations of the bridge in case of $\alpha=1.0$ are the smallest. This indicates that, for the high-pier bridge system concerned in this work, the optimal damping exponent α should be set to 1.0.
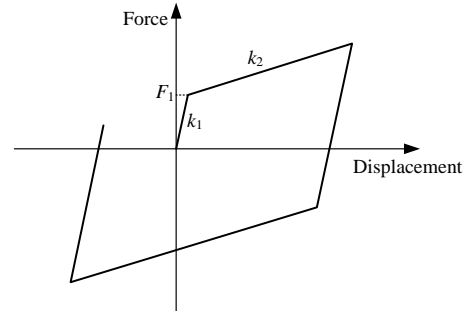
(2) Determination of damping coefficient C

In the cases of $\alpha=1.0$, the vibration reduction rates (VRRs) of VD in different bridge systems are displayed in Fig. 10.

As seen from the figure, when the damping of the damper increases from 0 to 15000 kN·s/m, the largest VRRs appear with different damping values in different calculation conditions. For 40 m-high bridge, the optimal damping is calculated to be about 3199 kN·s/m and 1063 kN·s/m subject to No. 1 earthquake and No. 2 earthquake, respectively. For 50 m-high bridge, the values are 3100 kN·s/m and 940 kN·s/m subject to these two earthquakes. Furthermore, for bridge system with 60 m-high pier, the

optimal damping is determined to be about 2483 kN·s/m and 2927 kN·s/m excited by No. 1 earthquake and No. 2 earthquake. In fact, subject to the other 6 earthquake samples, the optimal damping of VD in bridge systems with different pier-heights also changes in the range of 950 kN·s/m and 3500 kN·s/m. Thus, in this research, the values of 1000 kN·s/m and 3000 kN·s/m are selected as the optimal damping of VD in the following assessments and comparisons.

4.2 Optimal parameters of FPB

FPBs are increasingly employed because of their special features such as the stability of the physical properties and durability (Landi *et al.* 2016), which combine frictional steel sliding surfaces. Through the pendular motion of the slider on a perfectly spherical surface, the device is able to recenter by itself and dissipate a lot of energy through the sliding motions on the curved surface. The bilinear mechanics characteristic of a FPB is shown in Fig. 11, where, k_1 and k_2 are the slopes of the bilinear curve.

According to the design methodology of FPB, several parameters should be determined before finally designing a FPB, including:
• vertical force (caused by dead load) applying on the bearing (W);
• cutting force of the anti-sliding bolts (F_c);
• the first-order natural vibration frequency or vibration period of the bridge.

(1) Vertical force applied on the bearing

This vertical force W is caused by dead load of the structure, which consists of the secondary dead load and the self-weight of the bridge. According to the design drawing of the 32.6 m-long T-beam bridge, the secondary dead load is 160 kN/m, and the self-weight is 587.34 t. Thus, the
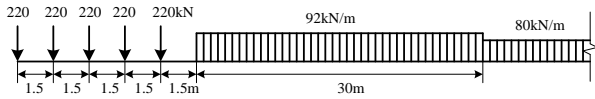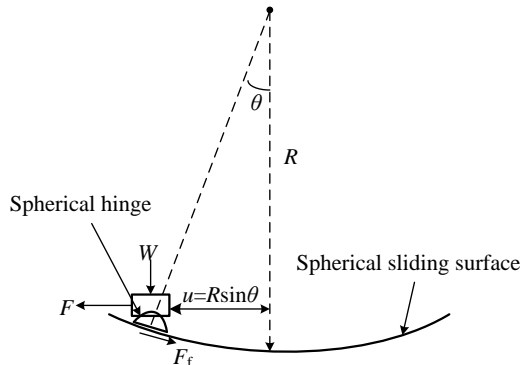
Fig. 12 China railway standard live loading

Fig. 13 Motion mechanism of FPBs

vertical force applying on each FPB is 1373 kN.

(2) Cutting force of the anti-sliding bolts

In the design stage, the cutting force F_c can be expressed by

$$F_c = \lambda \cdot F_b \qquad (4)$$

where, F_b is the maximum braking force, and λ is the safety coefficient. According to the research in literature (Zhuang 2012), λ can be set to 1.3. Thus, to determine F_c, the braking force should be investigated firstly.

Based on the description in China's current code "Fundamental code for design on railway bridge and culvert (TB10002.1-2005)", the braking force can be set to 10% of the vertical static live load F_v. Also, according to the same code, China railway standard live loading is shown in Fig. 12.

Employing the live loading in Fig. 12, F_v can be calculated to be 3409.2 kN, and then F_b is set to be 341 kN. Further, the cutting force F_c is calculated to be 443.3 kN.

(3) First-order natural vibration frequency or vibration period

The first-order natural vibration frequencies of the bridges can be obtained by carrying out modal analysis employing the established finite element models. Finally, the first-order frequencies in lateral direction for 40 m-height, 50 m-height, and 60 m-height bridges are 3.6 Hz, 2.49 Hz, and 1.81 Hz, respectively. The corresponding vibration periods are 0.28 s, 0.4 s, and 0.55 s, respectively. The motion mechanism of FPB is shown in Fig. 13.

In Fig. 13, W is the vertical force applying on the FPB, F_f is the friction force, and F is the lateral force of the bearing, which can be expressed as

$$F = W \tan \theta + \frac{F_f}{\cos \theta} \qquad (5)$$

Table 3 Parameters of the designed FPBs

Parameter	40 m-height bridge	50 m-height bridge	60 m-height bridge	Unit
T	0.84	1.2	1.65	s
R	0.2	0.36	0.7	m
k_1	4.43×10^8	4.43×10^8	4.43×10^8	N/m
k_2	6.87×10^6	3.81×10^6	1.96×10^6	N/m

in which, $W\tan\theta$ is caused by restoring force, and $F_f/\cos\theta$ is caused by friction force. Usually, the pendulum angle θ is relatively small, thus, $\cos\theta \approx 1$.

On this basis, the stiffness k_1 and k_2 in Fig. 11(b) can be written by

$$k_1 = \frac{F_c}{d_c} \qquad (6)$$

$$k_2 = \frac{W\tan\theta}{u} = \frac{W}{R\cos\theta} \approx \frac{W}{R} \qquad (7)$$

in Eq. (6), F_c is the cutting force of the anti-sliding bolts, which is determined in the above calculations; d_c is the displacement when the bolts are cut out, and this value is set to be 0.001 m in this study.

Further, the isolation period of a FPB can be expressed by

$$T = 2\pi\sqrt{\frac{W}{k_2 g}} = 2\pi\sqrt{\frac{R}{g}} \qquad (8)$$

And the radius of the spherical sliding surface is written as

$$R = \left(\frac{T}{2\pi}\right)^2 g \qquad (9)$$

To calculate the radius of the sliding surface, the isolation period T should be determined firstly. From the design methodology of FPB (Zhuang 2012), the isolation period can be set to 2-4 times the first-order vibration period of the bridge structure without SVR measures. Thus, for 40 m-height, 50 m-height, and 60 m-height bridges, the isolation periods are set to be 0.84 s, 1.2 s, and 1.65 s, respectively. Further, based on Eqs. (6), (7), and (9), the FPBs for all the bridge systems are designed, whose parameters are listed in Table 3.

4.3 Optimal parameters of TMD

Before finally determining the optimal parameters for TMD, it should be noticed that natural frequencies of bridges are very important based on the design methodologies of TMD. However, the natural frequencies are sensitive to temperature changing below the freezing point. In this research, the temperature effect is not considered due to the following two reasons:
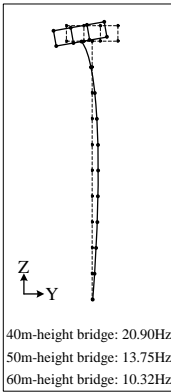
(a) In some practical cases, adaptive TMDs or multi-TMDs are used to eliminate the temperature effect. However, the adaptive TMDs and multi-TMDs will sharply
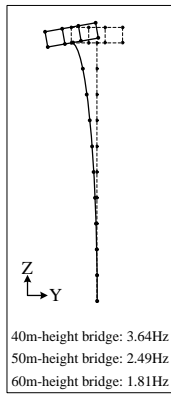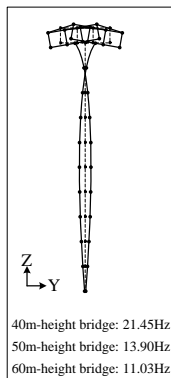
(a) 1st-order bending mode of piers (two piers move in the same direction)
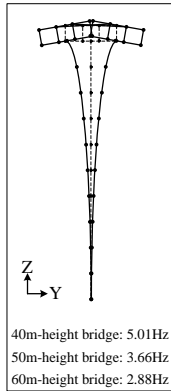
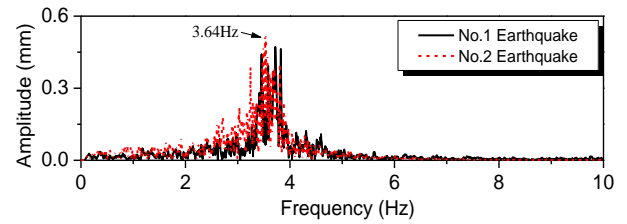(b) 1st-order bending mode of piers (two piers move in opposite directions)

(c) 2nd-order bending mode of piers (two piers move in the same direction)
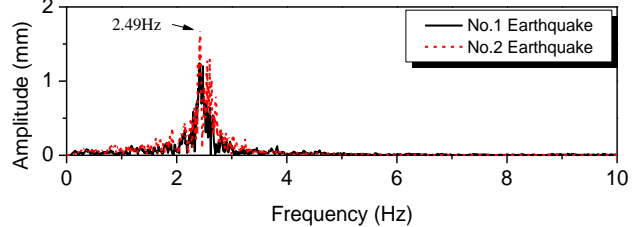

(d) 2nd-order bending mode of piers (two piers move in opposite directions)
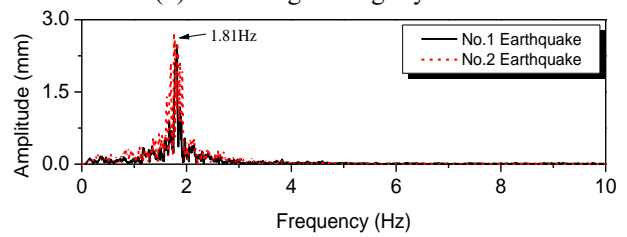
Fig. 14 Modal analysis results

(a) 40 m-height bridge system

(b) 50 m-height bridge system

(c) 60 m-height bridge system

Fig. 15 Displacement of pier-top in frequency domain

increase the cost due to numerous high-pier bridges in this railway line, which can only be employed in some special long-span bridges. While for the common 32.6 m-long T-beam bridges, comprehensively considering the cost and vibration reduction effect, one single TMD is designed on each high-pier.

(b) According to "Fundamental code for design on railway bridge and culvert (TB10002.1-2005)" published by the Ministry of Railways in China, the average temperatures along Sichuan-Tibet Railway in summer and winter are 24°C and 2°C respectively, which indicates that the temperature nearby the railway line changes gently in one year, and the influence of temperature on natural frequency is relatively small.

Based on Den Hartog's research (Den Hartog 1956), TMD can be designed according to the following equations

$$
\begin{cases}
\mu = \dfrac{m}{M} \\[2mm]
k = m\dfrac{K}{M}\left(\dfrac{1}{1+\mu}\right)^2 \\[2mm]
c = 2m\sqrt{\dfrac{K}{M}}\sqrt{\dfrac{3\mu}{8(1+\mu)^3}}
\end{cases}
\tag{10}
$$

in which, m, c, k are the mass, the stiffness and the damping of the TMD system, respectively; M and K are the mass and the stiffness of the bridge system, respectively; μ is the mass ratio. It should be stated that bridges are continuous flexible beams, and TMDs are designed to absorb vibrations in the specific vibration modes. That is to say, M and K are

Fig. 16 Actual structure on the pier-top of the T-beam bridge

Table 4 Parameters of the designed TMDs

Parameter	40 m-height bridge	50 m-height bridge	60 m-height bridge	Unit
m	85.7	85.7	85.7	t
μ	0.051	0.04	0.036	--
k	39.7	19	8.83	MN/m
c	399	304	168	kN·s/m

Note: these parameters are designed based on the first order bending mode of high-piers

the modal mass and the modal stiffness of the bridge in one certain frequency, which can be calculated by equivalent mass identification method (Zhu *et al.* 2015, 2017a).

To design a perfect TMD according to the design methodology, two issues should be addressed seriously, including a) the excited vibration mode of the primary structure, and b) the mass ratio. The following calculations are conducted to solve the problems.

(1) Excited vibration mode of high-pier bridge

As known from the design methodology of TMD, the excited vibration modes of the high-pier bridges must be determined primarily, which should be restrained. In order to achieve this goal, modal analysis and dynamic analysis are conducted employing the established bridge models, and the results are illustrated in Figs. 14-15.

As obviously seen from Figs. 14-15, for the bridges with different piers, only the first-order bending modes of the piers (two piers move in the same direction) are excited by different earthquake samples. That is to say, for all the concerned high-pier bridges, the TMDs should be designed according to the first-order bending modes of the piers. At the same time, in the first-order bending mode of piers, the modal displacements of the pier-tops are the largest. Thus, the TMDs should be further installed on the pier-tops.

(2) Determination of mass ratio

As seen from Eq. (10), the mass ratio μ is a key parameter, which should be determined before calculating k and c. In practical situation, the mass ratio is related to the installation space, thus, the installation space for TMD at pier-top is also evaluated. Fig. 16 shows the actual situation on the pier-top of the T-beam bridge, and it can be seen
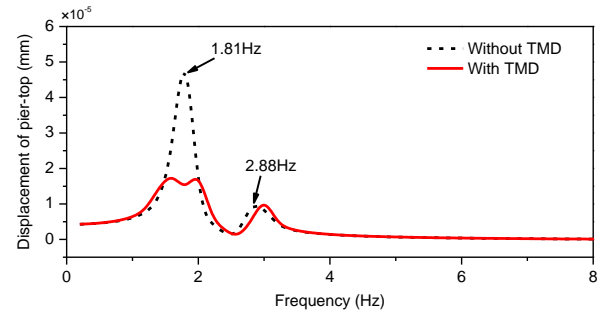

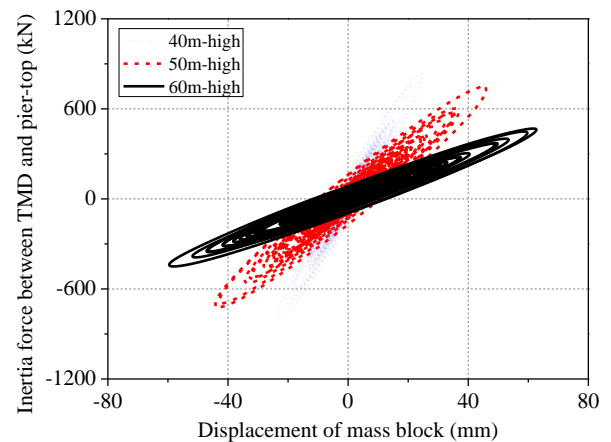Fig. 17 Displacement of pier-top with and without TMD in frequency domain

Fig. 18 Relationship between the peak displacement of mass block and the inertia force of TMD-pier

visually that there is a lot of space on the pier-top. According to the design drawing, the rest space is calculated to be almost 15.6 m³. Taking the TMD installation and other accessory structures on the top of the pier into consideration, a space reduction coefficient of 30% is employed, and the volume of the mass block is finally determined to be 10.92 m³. To make the mass block of the TMD heavier, the material of the mass block is chosen as steel, whose density is 7850 kg/m³. As a result, the weight of the mass block is calculated to be 85.7 t.

The excited vibration mode and the mass of the mass block are figured out in the above analysis. Further, according to the TMD design theory, the parameters of TMDs are listed in Table 4.

To verify whether the determined parameters of TMDs are the optimal, a harmonic response analysis is conducted. Taking the 60 m-height bridge system as an example, the displacements of pier-top with and without TMD in frequency domain are illustrated in Fig. 17.

It can be clearly seen that the vibration in 1.81Hz (i.e. first-order bending modes of the piers) is obviously decreased to a very small level. Moreover, the result with TMD satisfies the fix-point principle (Hahnkamm 1933). This indicates that: (a) the designed TMD is effective to reduce seismic responses of bridge, and (b) the parameters of the designed TMD are the optimal.

Moreover, to further check the peak displacement of the mass block and the inertia force between TMD and pier-top,

Table 5 Variation of different indicators subject to No.1 Earthquake sample

Indicator	Height (m)	Without SVR measures	VD (1000 kN·s/m)	VD (3000 kN·s/m)	FPB	TMD
Displacement of pier-top (mm)	40	16.99	14.27	11.55	9.17	10.19
	50	32.04	27.43	30.09	17.18	19.29
	60	42.45	36.51	33.96	23.35	25.47
Acceleration of pier-top (m/s²)	40	9.85	8.97	7.78	9.26	7.49
	50	9.96	9.42	8.78	9.34	7.47
	60	9.58	9.21	8.14	9.01	7.19
Bending moment of pier-bottom (×10⁸N·m)	40	4.18	3.55	3.43	2.68	2.51
	50	4.98	4.42	4.68	3.19	3.05
	60	5.04	4.44	4.69	3.23	3.12
Stress of pier-bottom (MPa)	40	2.57	1.88	2.06	1.85	1.67
	50	3.25	2.31	2.39	2.28	2.05
	60	3.39	2.86	3.06	2.48	2.21

the dynamic responses of the designed TMDs subject to No. 1 earthquake, which is the strongest earthquake among all the selected samples, as seen in Fig. 18.

As seen from Fig. 18, with the pier-height increases, the displacement of mass block relative to pier-top increases, while the inertia force between TMD and pier-top decreases. Excited by the No. 1 earthquake sample, the displacement of mass block relative to pier-top varies from 25 mm to 60 mm when the pier-height changes from 40 m to 60 m, indicating that the rest space on the pier-top is enough for the small-range move of the designed TMDs. Furthermore, the inertia force between TMD and pier-top changes in the range of 550 kN and 900 kN, which indicates the TMDs can be installed firmly on the pier-top with large-size bolts.

5. Dynamic assessment of different SVR measures

The optimal parameters of the selected three SVR measures are investigated in the previous section, and in this part, the dynamic assessment and comparison are conducted employing these designed SVR measures.

Adopting different SVR measures, the selected four indicators, namely displacement of pier-top, acceleration of pier-top, bending moment of pier-bottom and the stress of pier-bottom, are investigated subject to different earthquake samples. Table 5 lists the change of different indicators subject to No.1 earthquake sample. As seen from the table, these indicators are obviously reduced by different SVR measures compared with the results without measures. Also, it should be stated that some indicators exceed their limits subject to No. 1 earthquake in some cases, and this is because the No. 1 earthquake sample is the strongest earthquakes among the selected 8 samples. Further, to intuitively investigate the vibration reduction effects of different measures, VRRs for different indicators are calculated.

The vibration reduction effects of different SVR measures subject to No. 1 and No. 2 earthquake samples are illustrated in Figs. 19 and 20. As seen from these results, VRRs for the selected four dynamic indicators (i.e., displacement, acceleration, moment and stress of the pier) are obvious, indicating that the dynamic vibrations of the whole bridge system are reduced, and all the measures can be used to reduce the seismic vibrations in different degrees. The displacements of pier-top are most sensitive to the adopted SVR measures, while the accelerations of pier-

(a) Displacement of pier-top

(b) Acceleration of pier-top
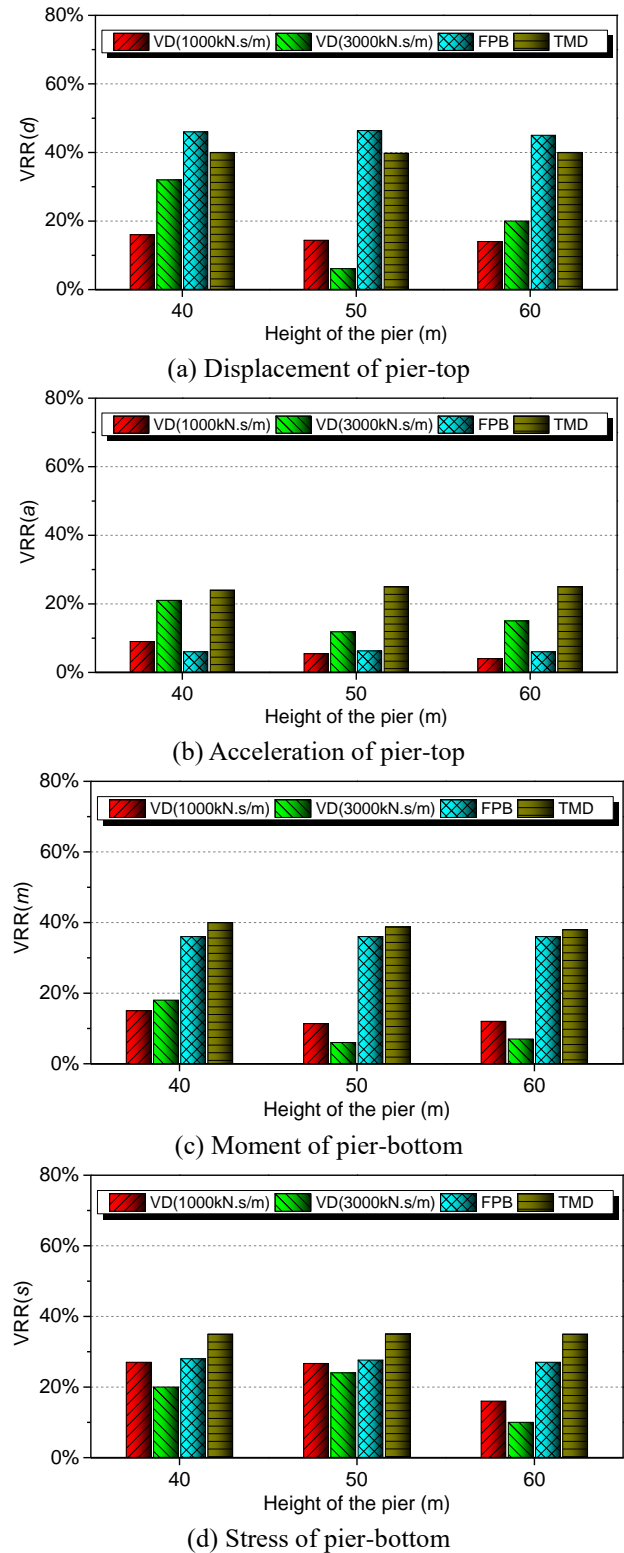
(c) Moment of pier-bottom

(d) Stress of pier-bottom

Fig. 19 Dynamic assessment of different SVR measures subject to No. 1 Earthquake

top are worst. When the height of the piers increases, the vibration reduction effects are almost the same, indicating that the height of pier almost has no influence on the SVR effects.

Additionally, the vibration reduction effects subject to other 6 earthquake samples show the similar results to the
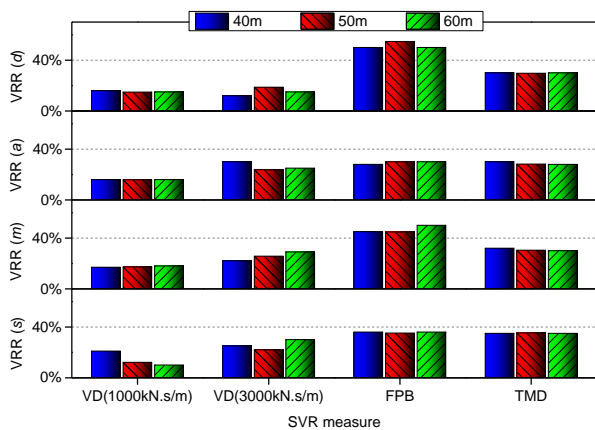
Fig. 20 Dynamic assessment of different SVR measures subject to No. 2 Earthquake

above results. Thus, these results are not illustrated in this work due to space limitations. Moreover, for different earthquake samples and different indicators, the vibration reduction effects are different. As a whole, with regard to the bridge structures concerned in this present work, among all the investigated measures, the vibration reduction effect of VD is weaker than that of the other two measures.

Meanwhile, the SVR effects of FPB and TMD are almost the same.

Although from the perspective of vibration reduction effects, there is no big difference between FPB and TMD, comprehensively considering their installation and maintenance, the SVR measure of TMD is a better choice to absorb vibration caused by earthquakes in the authors' opinion. The reasons are listed below:

(a) For the existing high-pier bridges with common bearings, it is easier to install TMDs on the pier-tops than to exchange the bearings.

(b) For a certain bridge, a large earthquake may break the bearing systems, so the FPBs need to be replaced with new ones after a great earthquake, which costs a lot. Relatively, TMDs are durable and hard to be damaged.

(c) The TMD is designed to restrain the first vibration mode of the high-pier in lateral direction, which is most likely to be excited, indicating the designed TMD can also reduce vibrations of the high-pier under other excitations (e.g., running trains), not merely the earthquake loadings. That is to say, TMD has a wider range of application areas than FPB.

In this aspect, for the concerned high-pier T-beam bridges in Sichuan-Tibet Railway, the best SVR measure is TMD according to the investigation in this present work.

6. Conclusions

To reduce seismic vibrations of common 32.6 m-long high-pier T-beam bridges in Sichuan-Tibet Railway, this paper has proposed an investigation on determining the optimal parameters of different SVR measures, including viscous dampers, friction pendulum bearings, and tuned mass dampers. Then, the vibration reduction effects of different measures have been evaluated, and finally, the

most appropriate SVR measure for high-pier bridges in Sichuan-Tibet Railway is determined. From this study, the following conclusions can be reached:

(1) All the investigated SVR measures are effective to reduce vibration of high-pier bridges subject to earthquakes.

(2) The optimal parameters for FPB and TMD are only related to the bridge structures, while the optimum values for VD vary with different bridge structures and different excitations.

(3) For high-pier bridges with different heights, the vibration reduction effects of all the selected measures are almost the same, indicating that the height of pier has little effects on the performances of SVR measures.

(4) Comprehensively considering the vibration absorption performance, the installation and maintenance, for the bridge structures concerned in this paper, TMD is most reasonable and economic to absorb vibrations caused by earthquakes among all the adopted measures in this paper.

It should be stated that, in this research, the parameters of the bridge, the pier and the foundation are deterministic. In further works, the sensitivity of these parameters on the performance of different SVR measures will be investigated.

Acknowledgments

References

Brock, J.E. (1946), "A note on the damped vibration absorber", *J. Appl. Mech.*, **13**(4), A-284.

Buckle, I.G. (1986), "Development and application of base isolation and passive energy dissipation: A world overview", *Appl. Technol. Council Rep.*, **17**, 153-174.

Buckle, I.G. and Mayes, R.L. (1990), "Seismic isolation: History, application, and performance-a world view", *Earthq. Spectr.*, **6**(2), 161-201.

Ceravolo, R., Demarie, G.V. and Giordano, L. (2009), "Problems in applying code-specified capacity design procedures to seismic design of tall piers", *Eng. Struct.*, **31**(8), 1811-1821.

Chen, Z., Fang, H., Ke, X. and Zeng, Y. (2016), "A new method to identify bridge bearing damage based on radial basis function neural network", *Earthq. Struct.*, **11**(5), 841-859.

Chen, Z., Zhai, W. and Tian, G. (2018a), "Study on the safe value of multi-pier settlement for simply supported bridges in high-speed railways", *Struct. Infrastruct. E.*, **14**(3), 400-410.

Chen, Z., Zhai, W. and Yin, Q. (2018b), "Analysis of structural stresses of tracks and vehicle dynamic responses in train-track-bridge system with pier settlement", *P. I. Mech. Eng. F-J. Rail*, **232**(2), 421-434.

Chen, Z., Zhai, W., Cai, C. and Sun, Y. (2015), "Safety threshold of high-speed railway pier settlement based on train-track-bridge dynamic interaction", *Sci. Chin. Technol. Sci.*, **58**(2), 202-210.

Den Hartog, J.P. (1956), *Mechanical Vibrations*, 4th Edition, McGraw-Hill.

Fenz, D.M. and Constantinou, M.C. (2006), "Behaviour of the double concave friction pendulum bearing", *Earthq. Eng. Struct. D.*, **35**(11), 1403-1424.

Frýba, L. (1976), "Nonstationary response of a beam to moving random force", *J. Sound Vibr.*, **46**(3), 323-338.

Geology Institute of China Earthquake Administration (2013), *Report on the Evaluation of Fault Activity along the Lhasa-Nyingchi Section Project of the Chuanzang Railway and the Regionalization of Ground Oscillation Parameters*.

Hahnkamm, E. (1933), "Die dämpfung von fundamentschwingungen bei veränderlicher erregerfrequenz", *Arch. Appl. Mech.*, **4**(2), 192-201.

Hüffmann, G.K. (1985), "Full base isolation for earthquake protection by helical springs and viscodampers", *Nucl. Eng. Des.*, **84**(3), 331-338.

Kelly, J.M. (1988), *Base Isolation in Japan*, Earthquake Engineering Research Center, College of Engineering, University of California, U.S.A.

Landi, L., Grazi, G. and Diotallevi, P.P. (2016), "Comparison of different models for friction pendulum isolators in structures subjected to horizontal and vertical ground motions", *Soil D. Earthq. Eng.*, **81**, 75-83.

Main, J.A. and Jones, N.P. (2002), "Free vibrations of taut cable with attached damper. I: Linear viscous damper", *ASCE J. Eng. Mech.*, **128**(10), 1062-1071.

Mokha, A., Constantinou, M. and Reinhorn, A. (1990), "Teflon bearings in base isolation I: Testing", *ASCE J. Struct. Eng.*, **116**(2), 438-454.

Ormondroyd, J. (1928), "Theory of the dynamic vibration absorber", *Trans. ASME*, **50**, 9-22.

Pacheco, B.M., Fujino, Y. and Sulekh, A. (1993), "Estimation curve for modal damping in stay cables with viscous damper", *ASCE J. Struct. Eng.*, **119**(6), 1961-1979.

Quaranta, G., Mollaioli, F. and Monti, G. (2016), "Effectiveness of design procedures for linear TMD installed on inelastic structures under pulse-like ground motion", *Earthq. Struct.*, **10**(1), 239-260.

Sladek, J.R. and Klingner, R.E. (1983), "Effect of tuned-mass dampers on seismic response", *ASCE J. Struct. Eng.*, **109**(8), 2004-2009.

Soto-Brito, R. and Ruiz, S.E. (1999), "Influence of ground motion intensity on the effectiveness of tuned mass dampers", *Earthq. Eng. Struct. D.*, **28**(11), 1255-1271.

Timoshenko, S. (1922), "On the forced vibrations of bridges", *Philosoph. Mag. Ser.*, **6**, 1018-1019.

Veletsos, A.S. and Ventura, C.E. (1986), "Modal analysis of non-classically damped linear systems", *Earthq. Eng. Struct. D.*, **14**(2), 217-243.

Zayas, V.A., Low, S.A. and Mahin, S.A. (1987), *The FPS Earthquake Resisting System Experimental Report*, Earthquake Engineering Research Center.

Zhu, S., Wang, J. and Cai, C. (2017b), "Development of a vibration attenuation track at low frequencies for urban rail transit", *Comput.-Aid. Civil Inf.*, **32**(9), 713-726.

Zhu, S., Yang, J. and Cai, C. (2017a), "Application of dynamic vibration absorbers in designing a vibration isolation track at low-frequency domain", *P. I. Mech. Eng. F-J. Rail*, **231**(5), 546-557.

Zhu, S., Yang, J. and Yan, H. (2015), "Low-frequency vibration control of floating slab tracks using dynamic vibration absorbers", *Vehic. Syst. Dyn.*, **53**(9), 1296-1314.

Zhuang, J.S. (2012), *Seismic Isolation Bearings for Bridges*, China Railway Publishing House, Beijing, China.

CC